Leckie, R.M., Sigurdsson, H., Acton, G.D., and Draper, G. (Eds.), 2000
Proceedings of the Ocean Drilling Program, Scientific Results, Vol. 165

16. ALKENONE UNSATURATION ESTIMATES OF SEA-SURFACE TEMPERATURES AT SITE 1002 OVER A FULL GLACIAL CYCLE[1]

Timothy D. Herbert[2] and Jeffrey D. Schuffert[2,3]

ABSTRACT

We determined alkenone concentrations (µg/g dry sediment) and unsaturation indices ($U^{k'}_{37}$) on 280 samples from Ocean Drilling Program Hole 1002C over the last full glacial cycle (marine oxygen isotope Stages [MIS] 1–6). Alkenone concentrations vary dramatically in relation to glacial–interglacial cycles, with high concentrations typical of interglacial stages, high sea level, inferred high surface productivity, and bottom-water anoxia. Our reconstruction of low productivity during the last glacial maximum is consistent with previous reports of a sharp decline in the foraminiferal species *Neogloboquadrina dutertrei,* an upwelling index. Alkenone paleotemperatures show little cooling at both the last glacial maximum and MIS 6. Variations of as much as 4°C occurred during the earlier part of MIS 3 and MIS 4 as well as the latter part of MIS 5. The absence of cooling during glacial maxima determined from alkenone paleothermometry is consistent with faunal reconstructions for the western Caribbean but requires that much of the oxygen isotopic record of the planktonic foraminifer *Globigerinoides ruber* be influenced by salinity variations rather than temperature.

INTRODUCTION

As noted elsewhere in this volume, Ocean Drilling Program (ODP) Site 1002 offers an unusual chance to study tropical climate and paleoceanography at high resolution over many of the late Pleistocene cycles of global ice volume and sea-level change. Data recovered from Site 1002 will help to assess the stability of tropical sea-surface temperatures (SST) on glacial–interglacial time scales and the effects of changes in sea level on oxygenation and carbon burial in the silled Cariaco Basin. In particular, the Cariaco Basin sediments may provide an unusual archive to assess the controversial topic of glacial sea-surface cooling during ice volume maxima (CLIMAP, 1976, 1984; Rind and Peteet, 1985; Broecker, 1986; Mix et al., 1986; Guilderson et al., 1994; Stott and Tang, 1996) and to determine the extent to which millenial-scale climate oscillations such as the Younger Dryas and Dansgaard-Oeschger Events from the North Atlantic (Bond et al., 1993) penetrated to the tropics (Hughen et al., 1996; Curry and Oppo, 1997). Previous work from piston cores has focused on the details of oxygenation, oxygen isotopic, and productivity history from the last glacial maximum (LGM) through the Holocene (Peterson et al., 1991; Hughen et al., 1996; Lin et al., 1997). We discuss here the significance of SST estimates derived from the $U^{k'}_{37}$ biomarker approach over a full glacial to interglacial cycle.

The $U^{k'}_{37}$ ("alkenone") approach estimates paleotemperatures by measuring the unsaturation index of di- and triunsaturated C_{37} ketones synthesized by several species of haptophyte algae, of which *Emiliania huxleyi* and *Gephyrocapsa oceanica* are believed to be the most important (Volkman et al., 1980, 1995; Marlowe et al., 1984; Lesley et al., 1996). Field and culture studies have defined calibration functions relating the unsaturation index, expressed as

$$U^{k'}_{37} = C_{37:2}/(C_{37:2} + C_{37:3})$$

(Prahl et al., 1988), to growth temperature (Prahl and Wakeham, 1987; Prahl et al., 1988; Brassell, 1993). For this study, we use the Prahl et al. (1988) calibration derived from cultures of *E. huxleyi.* Core-top studies show that this relationship provides a good fit with a global database comparing unsaturation index to surface-water temperatures (Sikes et al., 1991; Rossell-Mele et al., 1994; Sonzogni et al., 1997; Herbert et al., 1998; Müller et al., 1998). We also discuss trends in the amount of alkenones preserved in Site 1002 sediments as an index of a combination of haptophyte productivity and bottom-water oxygenation. Data reported here provide a high-resolution (~500-yr sampling rate) look at the alkenone record over the last full glacial cycle.

HYDROGRAPHIC CONSIDERATIONS

The vertical and seasonal structure of gradients in temperature, salinity, nutrients, and light penetration in the Cariaco Basin will govern the distribution of haptophyte production in the upper water column and determine the value of the $U^{k'}_{37}$ recorded by underlying sediments. Consideration of modern hydrography helps clarify the meaning of late Holocene values of $U^{k'}_{37}$. Hydrography also provides a lens to interpret past variations in $U^{k'}_{37}$ and other indices of paleo-SST such as planktonic $\delta^{18}O$ and faunal assemblages. The important considerations for interpreting variations in the organic index include the vertical range of haptophyte growth in relation to thermal gradients and seasonal variations in the flux of haptophyte-produced alkenones from the euphotic zone to the seafloor.

Time-series data provided by F. Müller-Karger (pers. comm., 1997) in the Cariaco Basin not far from ODP Site 1002 characterize mean annual and seasonal variations in temperature and salinity in the basin. These data are consistent with previous "snapshot" pictures of Cariaco Basin hydrography (cf. Herrera and Febres-Ortega, 1975, cited by Peterson et al. [Chap. 4, this volume]; Lin et al., 1997) but provide a more representative picture of seasonal variance through the upper water column. We modeled the mean annual and seasonal variations in temperature and salinity by fitting the data at 10-m depth intervals to an equation representing a mean plus annual and first harmonic of the annual cycles (cosine wave) with mean amplitudes and phases of the cycles determined by least-squares regression. The addition of the first harmonic term made little difference to the range of

[1]Leckie, R.M., Sigurdsson, H., Acton, G.D., and Draper, G. (Eds.), 2000. *Proc. ODP, Sci. Results,* 165: College Station, TX (Ocean Drilling Program).
[2]Department of Geological Sciences, Box 1846, Brown University, Providence, RI 02912, U.S.A. timothy_herbert@brown.edu
[3]GEOMAR Research Center, University of Kiel, Wischhofstrasse 1-3, Building 4, D-24148 Kiel, Federal Republic of Germany.

temperatures calculated at most depths, but it significantly improved the fit to salinity. Figure 1 shows the application of this model to temperature at 2 m, which we consider SST. Clearly, because of the limited duration of the data set, we cannot model interannual variations in hydrography that might affect paleoceanographic proxy data. Mean annual and seasonal variations in temperature and salinity with depth are presented in Figure 2. The sill depth at 146 m very nearly coincides with the base of the thermocline.

Our Hole 1002C core-top temperature estimate of 24.9°C (Table 1) based on the alkenone unsaturation index is in striking agreement with the mean annual SST in the Cariaco Basin, which we determined to average 25.1°C from the oceanographic time series. We also determined the $U^{k'}_{37}$ of eight surficial samples from box cores collected by the Plume-07 cruise to the Cariaco Basin in 1990. These data should represent the most recent sediment deposition in the basin and hence be more closely related temporally to historical hydrographic data than the ~600-yr-old near-surface sample from Hole 1002C. The eight box core samples give a mean $U^{k'}_{37}$ of 0.906, equivalent to 25.5°C, with a standard deviation equivalent to ±0.4°C. Alkenone production must therefore occur very near the sea surface under present conditions in the Cariaco Basin.

The coincidence of the alkenone temperature signal with mean annual conditions does not prove that there is no seasonality of production and sedimentation of these organic compounds or no potential depth bias to their temperature of production. The annual range at the sea surface is estimated to be 5.5°C, and at times subsurface temperatures reach core-top $U^{k'}_{37}$ temperatures. However, if we look at an enlarged view of the upper 100 m of the Cariaco site, we see that it is hard to reconcile alkenone temperature estimates with production below 25 m at any time of the year (Fig. 3). It also seems unlikely that the alkenone signal is produced dominantly during the upwelling season of winter to early spring, which should result in core-top temperatures of ~23°C. Mixed-layer depths are quite shallow according to the Müller-Karger time series: we calculated an average mixed-layer depth of 15.8 ± 7.2 m over the length of the series. The alkenone core-top temperature estimate, therefore, can be explained most simply as a reflection of production either within or just below the mixed layer, with perhaps a slight bias to postupwelling growth.

These considerations of present-day relationships set the stage to consider hydrographic factors that might influence the interpretation of $U^{k'}_{37}$ temperatures and the relationship of these temperature estimates to foraminiferal faunas and isotopic time series. First, it seems likely that alkenone paleotemperatures in the Cariaco location will not have a strong upwelling signal embedded in them. Changes in alkenone paleotemperatures at our sample resolution of ~500 yr should reflect decadal- to century-scale climate variations instead of seasonal changes. Second, of the three foraminiferal species analyzed by Lin et al. (1997) (*Neogloboquadrina dutertrei, Globigerina bulloides,* and *Globigerinoides ruber*), the conditions of alkenone production most closely approximate those of the foraminifer *G. ruber* in the modern environment, whose isotopic signal appears to represent production under mean annual mixed-layer conditions (Overpeck et al., 1989; Lin et al., 1997).

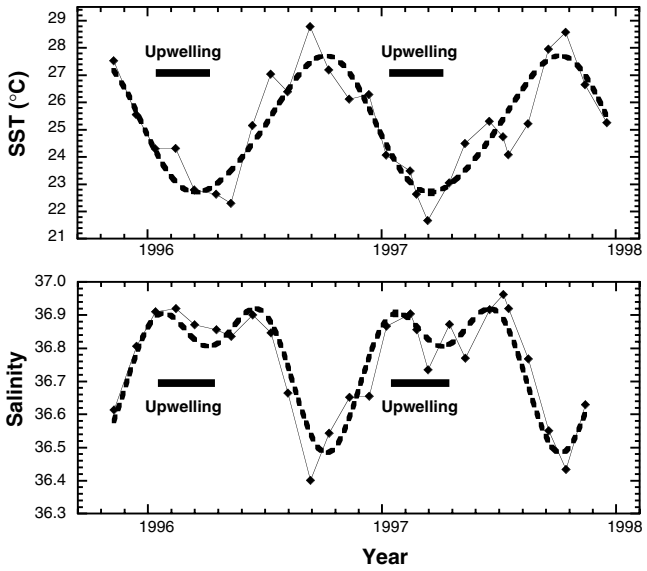

Figure 1. Time-series data from F. Müller-Karger (pers. comm., 1998) for surface temperatures and salinity in the Cariaco Basin (solid diamonds), fitted to a model of annual mean plus annual and semiannual cycles. SST = sea-surface temperatures. Solid horizontal bars indicate time of seasonal upwelling.

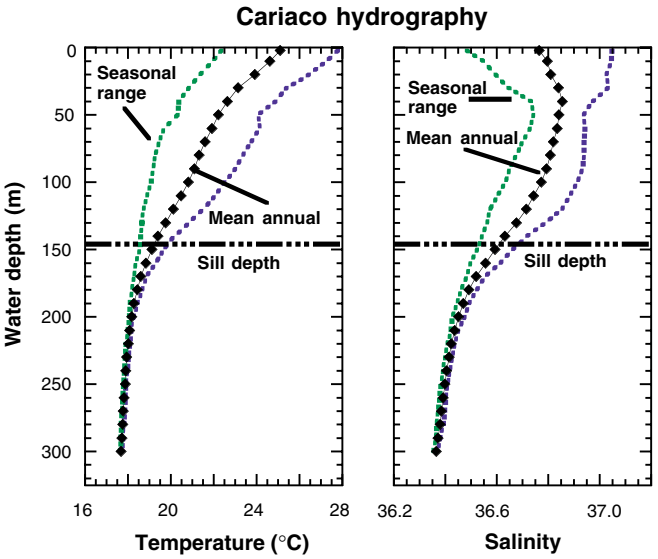

Figure 2. Vertical structure of Cariaco Basin upper water column derived from time-series data. The mean annual temperature and salinity structures are derived from the statistical fit to the annual mean. The seasonal range is defined as the sum of the amplitudes of the annual and semiannual terms (both high and low extremes) at each water depth.

METHODS

Samples (~0.5 g dry weight) were freeze dried and extracted in a 3:1 (v/v) methanol:hexane solution using an automated pressurized fluid extraction device (ASE 200, Dionex, Inc., Salt Lake City). This instrument exposes samples to small volumes of solvent at elevated pressure and temperature; it extracts organic compounds rapidly and delivers the extracts to annealed glass vials with polytetra-fluoroethylene (PTFE) septa. Extractions were carried out for 15 min at 150°C. Organic extracts were dried under a nitrogen stream before dilution for gas chromatography (GC). Although we generally avoid silica gel column treatment of extracts in our procedure, the complex makeup of Cariaco Basin lipid extracts forced us to use a short-column procedure. The column consisted of a Pasteur pipette packed with glass wool at the base. A silica gel column of ~3.75 cm was rinsed with methanol, methylene chloride, and hexane before loading organic extracts. Next, 50 µL of concentrated sample was transferred onto the column and eluted with 5.5 mL of methylene chloride.

Alkenone analyses employed gas chromatography (HP 5890) with flame-ionization detection. Samples were prepared using toluene as a solvent, and autosampler vials were sealed with PTFE septa to prevent the appearance of ghost peaks observed with rubber or silicone septa. The chromatographic column used was a J&W DB-1 (60-m length, 0.32-mm diameter, and 0.11-µm film thickness), with

Table 1. Results of alkenone analyses of Hole 1002C.

Core, section	Interval (cm)	Depth (mbsf)	Age (ka)	$U^{k'}_{37}$	Temperature (°C)	C_{37} ketones (mg/g)
1H-1	16-17	0.17	0.69	0.883	24.8	7.43
1H-1	36-37	0.37	1.14	0.901	25.4	4.51
1H-1	56-57	0.57	1.59	0.916	25.8	4.98
1H-1	74-75	0.75	1.99	0.905	25.5	6.14
1H-1	96-97	0.97	2.48	0.908	25.6	7.38
1H-1	116-117	1.17	2.93	0.914	25.7	5.39
1H-1	136-137	1.37	3.37	0.912	25.7	5.22
1H-2	16-17	1.67	4.04	0.914	25.7	3.71
1H-2	36-37	1.87	4.49	0.907	25.5	3.67
1H-2	56-57	2.07	4.94	0.905	25.5	4.67
1H-2	74-75	2.25	5.34	0.907	25.5	4.12
1H-2	96-97	2.47	5.84	0.915	25.8	3.65
1H-2	136-137	2.87	6.73	0.885	24.9	4.06
1H-3	16-17	3.17	7.40	0.893	25.1	3.20
1H-3	36-37	3.37	7.85	0.896	25.2	3.77
1H-3	56-57	3.57	8.29	0.880	24.7	4.25
1H-3	74-75	3.75	8.70	0.890	25.0	4.71
1H-3	96-97	3.96	9.18	0.882	24.8	6.98
1H-3	116-117	4.16	9.62	0.892	25.1	3.13
1H-3	136-137	4.36	10.07	0.873	24.5	2.38
1H-4	16-17	4.67	10.75	0.858	24.1	1.07
1H-4	36-37	4.87	11.20	0.871	24.5	2.10
1H-4	56-57	5.07	11.65	0.869	24.4	1.73
1H-4	74-75	5.25	12.05	0.873	24.5	2.46
1H-4	96-97	5.47	12.54	0.867	24.4	4.08
1H-4	116-117	5.67	12.99	0.852	23.9	5.57
1H-4	136-137	5.87	13.44	0.819	22.9	4.38
1H-5	16-17	6.17	13.88	0.822	23.0	3.02
1H-5	36-37	6.37	14.55	0.871	24.5	1.92
1H-5	56-57	6.57	14.86	0.913	25.7	0.57
1H-5	74-75	6.75	15.07	0.905	25.5	0.73
1H-5	96-97	6.97	15.34	0.893	25.1	0.13
1H-5	116-117	7.17	15.57			0.00
1H-5	136-137	7.37	15.81	0.897	25.2	0.05
1H-6	16-17	7.67	16.17	0.891	25.1	0.80
1H-6	33-34	7.84	16.37	0.878	24.7	0.42
1H-6	56-57	8.07	16.64	0.894	25.2	0.62
2H-1	16-17	8.57	17.07	0.884	24.9	0.53
2H-1	36-37	8.77	17.19	0.890	25.0	1.14
2H-1	56-57	8.97	17.31	0.878	24.7	0.88
2H-1	74-75	9.15	17.41	0.887	24.9	0.74
2H-1	96-97	9.37	17.55	0.886	24.9	0.61
2H-1	116-117	9.57	17.66	0.883	24.8	0.78
2H-1	136-137	9.77	17.78	0.869	24.4	1.36
2H-2	16-17	10.07	17.96	0.890	25.0	0.61
2H-2	36-37	10.27	18.08	0.883	24.8	0.80
2H-2	56-57	10.47	18.20	0.884	24.9	0.67
2H-2	74-75	10.65	18.30	0.878	24.7	0.71
2H-2	96-97	10.87	18.43	0.883	24.8	0.61
2H-2	116-117	11.07	18.55	0.873	24.5	0.80
2H-2	136-137	11.27	18.67	0.879	24.7	0.94
2H-3	16-17	11.57	18.85	0.880	24.7	0.67
2H-3	36-37	11.77	18.97	0.873	24.5	0.97
2H-3	56-57	11.97	19.08	0.878	24.7	0.91
2H-3	74-75	12.15	19.19	0.878	24.7	0.71
2H-3	96-97	12.37	19.32	0.882	24.8	0.92
2H-3	116-117	12.57	19.44	0.882	24.8	1.16
2H-3	136-137	12.77	19.56	0.896	25.2	0.93
2H-4	16-17	13.07	19.73	0.878	24.7	1.17
2H-4	36-37	13.27	19.85	0.891	25.1	1.39
2H-4	56-57	13.47	19.97	0.895	25.2	0.91
2H-4	74-75	13.65	20.01	0.889	25.0	1.17
2H-4	96-97	13.87	20.43	0.893	25.1	0.92
2H-4	116-117	14.07	20.82	0.885	24.9	1.21
2H-4	136-137	14.27	21.19	0.881	24.8	1.13
2H-5	16-17	14.57	21.76	0.883	24.8	0.63
2H-5	36-37	14.77	22.15	0.854	24.0	1.51
2H-5	56-57	14.97	22.52	0.869	24.4	0.64
2H-5	74-75	15.15	22.87	0.851	23.9	1.18
2H-5	96-97	15.37	23.30	0.858	24.1	1.08
2H-5	116-117	15.57	23.67	0.868	24.4	0.99
2H-5	136-137	15.77	24.06	0.873	24.5	1.20
2H-6	16-17	16.07	24.62	0.885	24.9	0.93
2H-6	33-34	16.24	24.94	0.879	24.7	0.70
2H-6	56-57	16.47	25.38	0.862	24.2	0.66
2H-6	74-75	16.65	25.73	0.873	24.5	0.90
2H-6	96-97	16.87	26.15	0.871	24.5	1.07
2H-6	116-117	17.07	26.54	0.866	24.3	1.21
2H-6	136-137	17.27	26.91	0.880	24.7	1.17
2H-7	16-17	17.57	27.47	0.885	24.9	2.85
2H-7	36-37	17.77	27.86	0.849	23.8	2.19
3H-1	6-7	17.97	28.68	0.864	24.3	1.18
3H-1	26-27	18.17	29.04	0.864	24.3	1.00
3H-1	46-47	18.37	29.42	0.873	24.5	1.23
3H-1	66-67	18.57	29.79	0.861	24.2	1.04
3H-1	86-87	18.77	30.17	0.873	24.5	1.62
3H-1	106-107	18.97	30.54	0.865	24.3	1.71
3H-1	126-127	19.17	30.92	0.824	23.1	2.02
3H-1	146-147	19.37	31.29	0.829	23.2	1.53
3H-2	6-7	19.47	31.48	0.849	23.8	3.27
3H-2	26-27	19.67	31.86	0.811	22.7	2.49
3H-2	66-67	20.07	32.61	0.818	22.9	1.51
3H-2	86-87	20.27	32.99	0.839	23.5	1.97
3H-2	106-107	20.47	33.36	0.794	22.2	2.76
3H-2	126-127	20.67	33.74	0.782	21.9	3.40
3H-2	144-145	20.85	34.07	0.832	23.3	1.55
3H-3	6-7	20.97	34.30	0.818	22.9	1.40
3H-3	26-27	21.17	34.67	0.862	24.2	1.72
3H-3	46-47	21.37	35.05	0.816	22.9	1.46
3H-3	66-67	21.57	35.43	0.819	22.9	1.54
3H-3	86-87	21.77	35.80	0.841	23.6	4.62
3H-3	106-107	21.97	36.18	0.803	22.5	3.59
3H-3	126-127	22.17	36.55	0.832	23.3	4.50
3H-4	6-7	22.50	37.17	0.845	23.7	1.39
3H-4	26-27	22.70	37.55	0.829	23.2	2.30
3H-4	46-47	22.90	37.92	0.851	23.9	1.83
3H-4	66-67	23.10	38.30	0.864	24.3	1.81
3H-4	86-87	23.30	38.42	0.860	24.2	5.57
3H-4	106-107	23.50	39.03	0.876	24.6	3.45
3H-4	126-127	23.70	39.62	0.844	23.7	4.01
3H-4	143-144	23.87	40.16	0.871	24.5	4.32
3H-5	6-7	24.00	40.57	0.801	22.4	3.73
3H-5	26-27	24.20	41.17	0.833	23.3	3.53
3H-5	46-47	24.40	41.81	0.838	23.5	2.82
3H-5	66-67	24.60	42.42	0.875	24.6	4.36
3H-5	86-87	24.80	43.04	0.847	23.8	3.40
3H-5	106-107	25.00	43.65	0.842	23.6	6.31
3H-5	126-127	25.20	44.27	0.876	24.6	1.50
3H-5	146-147	25.40	44.91	0.833	23.3	2.76
3H-6	6-7	25.53	45.30	0.864	24.3	4.27
3H-6	26-27	25.73	45.91	0.853	23.9	2.88
3H-6	46-47	25.93	46.53	0.816	22.9	2.41
3H-6	66-67	26.13	47.14	0.860	24.1	2.12
3H-6	86-87	26.33	47.75	0.868	24.4	2.55
3H-6	106-107	26.53	48.37	0.806	22.6	3.74
3H-6	126-127	26.73	48.98	0.777	21.7	2.44
3H-6	146-147	26.93	49.59	0.849	23.8	2.01
3H-7	6-7	27.03	49.92	0.844	23.7	1.80
3H-7	26-27	27.23	50.55	0.846	23.7	1.15
3H-7	46-47	27.43	51.15	0.825	23.1	1.97
4H-1	6-7	27.47	52.66	0.820	23.0	2.75
4H-1	26-27	27.67	53.25	0.799	22.4	4.04
4H-1	46-47	27.87	53.89	0.829	23.2	1.45
4H-1	73-74	28.14	54.70	0.876	24.6	1.22
4H-1	96-97	28.37	55.42	0.904	25.4	0.39
4H-1	116-117	28.57	56.04	0.846	23.7	0.52
4H-1	136-137	28.77	56.64	0.861	24.2	0.47
4H-2	6-7	28.97	57.25	0.893	25.1	0.47
4H-2	26-27	29.17	57.86	0.891	25.1	1.00
4H-2	46-47	29.37	58.48	0.873	24.5	1.13
4H-2	74-75	29.65	59.35	0.822	23.0	1.65
4H-2	96-97	29.87	60.00	0.827	23.2	1.03
4H-2	116-117	30.07	60.64	0.845	23.7	0.30
4H-2	136-137	30.27	61.26	0.874	24.6	0.71
4H-3	6-7	30.50	62.01	0.845	23.7	0.69
4H-3	26-27	30.70	62.41	0.839	23.5	1.09
4H-3	46-47	30.90	62.71	0.887	24.9	0.72
4H-3	73-74	31.17	64.00	0.864	24.3	2.06
4H-3	96-97	31.40	66.11	0.790	22.1	4.74
4H-3	116-117	31.60	66.94	0.824	23.1	2.24
4H-3	136-137	31.80	67.44	0.848	23.8	0.99
4H-4	6-7	32.07	68.46	0.807	22.6	1.67
4H-4	26-27	32.27	69.20	0.901	25.4	1.36
4H-4	46-47	32.47	69.76	0.783	21.9	5.66
4H-4	74-75	32.75	70.54	0.751	20.9	12.70
4H-4	96-97	32.97	71.49	0.821	23.0	6.11
4H-4	116-117	33.17	72.34	0.810	22.7	1.72
4H-4	136-137	33.37	73.19	0.853	24.0	1.06
4H-5	7-8	33.69	74.56	0.894	25.1	1.19
4H-5	26-27	33.88	75.37	0.797	22.3	4.33
4H-5	46-47	34.08	76.23	0.840	23.6	5.81
4H-5	73-74	34.35	77.39	0.786	22.0	10.16
4H-5	96-97	34.58	78.37	0.788	22.0	11.62
4H-5	116-117	34.78	79.23	0.865	24.3	7.89
4H-5	136-137	34.98	80.08	0.913	25.7	6.83
4H-6	7-8	35.22	81.11	0.920	25.9	5.54
4H-6	26-27	35.41	81.92	0.888	25.0	6.13
4H-6	46-47	35.61	82.78	0.814	22.8	6.27
4H-6	74-75	35.89	83.98	0.903	25.4	1.01
4H-6	96-97	36.11	84.92	0.902	25.4	0.41
4H-6	116-117	36.31	85.77	0.901	25.4	0.50
4H-6	136-137	36.51	86.63	0.896	25.2	0.80
4H-7	7-8	36.72	87.53	0.895	25.2	1.03
4H-7	26-27	36.91	88.34	0.869	24.4	3.57
4H-7	49-50	37.14	89.32	0.895	25.2	4.05
5H-1	6-7	36.97	89.80	0.921	26.0	5.18
5H-1	26-27	37.17	90.61	0.911	25.7	6.23
5H-1	46-47	37.37	91.42	0.924	26.0	7.01
5H-1	66-67	37.57	92.22	0.897	25.2	8.21
5H-1	86-87	37.77	93.00	0.909	25.6	7.95

Table 1 (continued).

Core, section	Interval (cm)	Depth (mbsf)	Age (ka)	$U^{k'}_{37}$	Temperature (°C)	C_{37} ketones (mg/g)
5H-1	106-107	37.97	93.78	0.905	25.5	6.59
5H-1	126-127	38.17	94.59	0.824	23.1	9.57
5H-1	144-145	38.35	95.31	0.792	22.1	11.71
5H-2	6-7	38.47	95.78	0.774	21.6	7.18
5H-2	26-27	38.67	96.58	0.847	23.8	6.48
5H-2	46-47	38.87	97.37	0.785	21.9	5.53
5H-2	66-67	39.07	98.18	0.754	21.0	6.86
5H-2	86-87	39.27	99.02	0.865	24.3	1.88
5H-2	106-107	39.47	99.82	0.906	25.5	1.28
5H-2	126-127	39.67	100.60	0.905	25.5	3.05
5H-2	146-147	39.87	101.40	0.900	25.3	2.85
5H-3	6-7	39.97	101.80	0.890	25.0	2.87
5H-3	26-27	40.17	102.60	0.904	25.4	2.71
5H-3	46-47	40.37	103.40	0.912	25.7	1.00
5H-3	66-67	40.57	104.19	0.920	25.9	1.03
5H-3	86-87	40.77	104.98	0.923	26.0	1.46
5H-3	106-107	40.97	105.78	0.918	25.9	3.09
5H-3	126-127	41.17	106.58	0.925	26.0	2.72
5H-3	143-144	41.34	107.25	0.930	26.2	2.88
5H-4	6-7	41.54	108.04	0.947	26.7	3.29
5H-4	26-27	41.74	108.83	0.957	27.0	3.13
5H-4	46-47	41.94	109.64	0.953	26.9	2.92
5H-4	66-67	42.14	110.44	0.957	27.0	3.49
5H-4	86-87	42.34	111.22	0.955	26.9	3.80
5H-4	106-107	42.54	112.01	0.961	27.1	3.51
5H-4	126-127	42.74	112.81	0.968	27.3	3.70
5H-4	145-146	42.93	113.57	0.958	27.0	4.35
5H-5	6-7	43.04	114.01	0.954	26.9	3.90
5H-5	26-27	43.24	114.81	0.939	26.5	4.60
5H-5	46-47	43.44	115.60	0.965	27.2	3.90
5H-5	66-67	43.64	116.41	0.964	27.2	4.11
5H-5	86-87	43.84	117.24	0.963	27.2	5.20
5H-5	106-107	44.04	118.03	0.953	26.9	3.97
5H-5	126-127	44.24	118.83	0.956	27.0	5.29
5H-5	142-143	44.40	119.47	0.950	26.8	5.78
5H-6	6-7	44.54	120.03	0.942	26.6	4.73
5H-6	26-27	44.74	120.83	0.943	26.6	2.69
5H-6	46-47	44.94	121.62	0.930	26.2	2.67
5H-6	66-67	45.14	122.42	0.934	26.3	2.18
5H-6	86-87	45.34	123.21	0.940	26.5	2.60
5H-6	106-107	45.54	124.01	0.926	26.1	1.66
5H-6	126-127	45.74	124.80	0.928	26.2	2.35
5H-6	145-146	45.93	125.56	0.915	25.8	1.98
5H-7	6-7	46.04	126.00	0.913	25.7	1.77
5H-7	26-27	46.24	126.80	0.870	24.5	1.90
5H-7	46-47	46.44	127.60	0.889	25.0	1.58
5H-7	66-67	46.64	128.40	0.896	25.2	1.27
5H-7	86-87	46.84	129.20	0.923	26.0	2.04
6H-1	6-7	46.47	130.51	0.935	26.3	1.23
6H-2	4-5	46.72	131.52	0.935	26.4	0.88
6H-2	26-27	46.94	132.40	0.934	26.3	2.15
6H-2	46-47	47.14	133.19	0.946	26.7	1.18
6H-2	66-67	47.34	133.97	0.951	26.8	1.93
6H-2	86-87	47.54	134.76	0.933	26.3	1.89
6H-2	106-107	47.74	135.56	0.932	26.3	0.61
6H-2	126-127	47.94	136.35	0.946	26.7	1.24
6H-2	142-143	48.10	136.97	0.938	26.4	0.91
6H-3	6-7	48.24	137.51	0.935	26.4	1.14
6H-3	26-27	48.44	138.31	0.932	26.3	0.90
6H-3	46-47	48.64	139.10	0.943	26.6	1.12
6H-3	66-67	48.84	139.90	0.931	26.2	0.44
6H-3	86-87	49.04	140.68	0.931	26.2	0.53
6H-3	106-107	49.24	141.46	0.921	25.9	0.54
6H-4	6-7	49.74	143.43	0.912	25.7	0.36
6H-4	25-26	49.93	144.19	0.913	25.7	0.59
6H-4	46-47	50.14	145.05	0.916	25.8	0.33
6H-4	66-67	50.34	145.87	0.917	25.8	0.62
6H-4	86-87	50.54	146.70	0.903	25.4	0.75
6H-4	106-107	50.74	147.52	0.911	25.6	0.38
6H-4	126-127	50.94	148.34	0.914	25.7	0.97
6H-4	143-144	51.11	149.02	0.900	25.3	0.36
6H-5	6-7	51.24	149.53	0.912	25.7	0.38
6H-5	28-29	51.46	150.39	0.908	25.6	0.48
6H-5	46-47	51.64	151.06	0.900	25.3	0.30
6H-5	66-67	51.84	151.79	0.895	25.2	0.33
6H-5	86-87	52.04	152.48	0.905	25.5	0.26
6H-5	106-107	52.24	153.14	0.904	25.4	0.50
6H-5	126-127	52.44	153.78	0.917	25.8	0.30
6H-5	145-146	52.63	154.35	0.923	26.0	0.31
6H-6	6-7	52.79	154.83	0.920	25.9	1.15
6H-6	26-27	52.99	155.39	0.932	26.3	1.47
6H-6	43-44	53.16	155.86	0.920	25.9	0.43
6H-6	66-67	53.39	156.48	0.915	25.8	0.65
6H-6	86-87	53.59	157.00	0.929	26.2	1.67
6H-6	106-107	53.79	157.52	0.913	25.7	0.55
6H-6	126-127	53.99	158.03	0.926	26.1	0.53
6H-6	143-144	54.16	158.46	0.915	25.8	1.22
6H-7	6-7	54.34	158.91	0.916	25.8	1.94
6H-7	26-27	54.54	159.41	0.909	25.6	1.82
6H-7	46-47	54.74	159.92	0.901	25.4	1.99
6H-7	66-67	54.94	160.44	0.905	25.5	2.37
6H-7	86-87	55.14	160.96	0.911	25.6	2.58
6H-7	106-107	55.34	161.50	0.921	25.9	2.12
6H-7	126-127	55.54	162.05	0.903	25.4	2.90
6H-7	146-147	55.74	162.60	0.902	25.4	2.68
6H-8	4-7	55.83	162.85	0.904	25.5	2.59
6H-8	26-27	56.04	163.44	0.912	25.7	2.67
6H-8	42-43	56.20	163.89	0.895	25.2	1.69
6H-8	65-66	56.43	164.55	0.903	25.4	1.51
6H-8	8-81	56.58	164.97	0.881	24.8	2.34

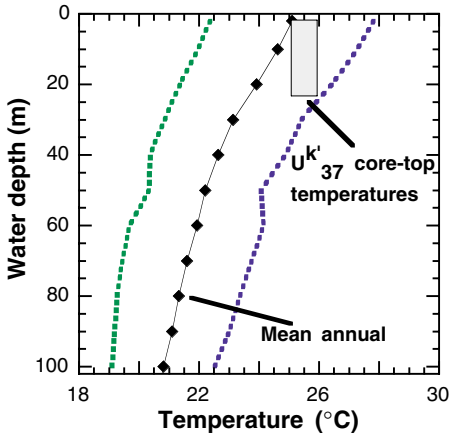

Figure 3. Comparison of upper water column temperature structure to the temperature estimate given by the $U^{k'}_{37}$ index determined in eight box core tops. Although a range of production scenarios describe the sediment data (shaded box represents range of $U^{k'}_{37}$ temperatures in core tops and possible depths of production in relation to annual variations in water-column temperature), the most plausible explanation involves alkenone synthesis near the sea surface with little seasonal bias. Dotted lines show high and low extremes.

a 10-m deactivated silica guard column on the injection side of the GC. Temperature programming was 12.5°C/min to 250°C followed by 1°C/min to 290°C, with an isothermal holding step at 320°C for 15 min. Calculation of the $U^{k'}_{37}$ index followed graphic determination of $C_{37:3}$ and $C_{37:2}$ peak areas using Hewlett-Packard Chemstation software. Quantification of abundance was achieved by adding C_{36} and C_{37} *n*-alkanes as external standards.

Paleotemperature estimates come from the Prahl et al. (1988) calibration of unsaturation index to growth temperature. We routinely achieved a reproducibility of better than ± 0.01 $U^{k'}_{37}$ units, as determined by multiple extractions of sediment standards from Santa Barbara Basin and the central California Margin. This corresponds to a nominal temperature uncertainty of <0.3°C using the Prahl et al. (1988) calibration, barring other complications in interpreting the unsaturation index. For several cases of very low alkenone concentrations (see Table 1), we re-extracted larger (2 g) quantities of sediment to ensure that the low alkenone concentration did not bias our gas chromatographic results. Reanalyses of these leaner samples yielded unsaturation indices identical to the initial values determined.

RESULTS

We examined the response of both alkenone concentrations, a proxy for haptophyte production and preservation, and alkenone

paleotemperature estimates across two glacial terminations. There is considerably more context in which to interpret the record of the last deglaciation (MIS 2–1 transition) because of greater supporting information on sea-level changes (Fairbanks, 1989), high-frequency global climate oscillations such as the Younger Dryas Event (Fairbanks, 1989), and previous studies from the Cariaco Basin (Hughen et al., 1996; Lin et al., 1997). The time scale for the results presented here comes from the isotope stratigraphy of Peterson et al. (Chap. 4, this volume) based on the planktonic foraminifer *G. ruber*. Because the *G. ruber* record clearly differs in detail from the global SPECMAP isotopic stack, we caution that the time scale may be somewhat less accurate than a chronology based on benthic $\delta^{18}O$ data representative of global ice-volume changes. We also note that the high-frequency variations seen in many intervals of both $\delta^{18}O$ and $U^{k'}_{37}$ records suggest that both time series are still undersampled and that it would be premature to compare isotopic and alkenone data too closely.

Although both alkenone concentrations and paleotemperatures display substantial variations over the last full glacial cycle in the Cariaco Basin, the alkenone concentration measurements resemble the oxygen isotopic record more than they resemble the paleotemperature data (Fig. 4). Alkenone concentrations vary positively both with ice volume and with total organic carbon (TOC) (Haug et al., 1998). The alkenone concentration record differs from the TOC record in that the amounts of long-chained ketones are higher on a relative basis during MIS 5 than are the TOC contents. The median alkenone quantity (4.4 µg/g) over the entire record is about one order of magnitude higher than is typical of pelagic sediments (cf. Prahl et al., 1989; Lyle et al., 1992) and is slightly higher than the average concentration of long-chained ketones at Santa Barbara Basin, another silled and frequently anoxic basin, over the same time interval (Herbert et al., 1995).

Alkenone paleotemperatures range from a high of 27.3°C during marine isotope Substage 5E to lows of 21.0°–22.0°C during brief intervals across the MIS 2–1 transition and during MIS 3–5 (Fig. 5). The mean temperature estimated for the entire record is 24.8°C, similar to modern core-top temperatures. MIS 3 and 4 and Substages 5A–5C contain high-frequency swings in estimated temperatures, with some estimates exceeding modern values juxtaposed with intervals as cold as 21°C. Both the LGM and Stage 6 intervals show very little cooling from Holocene and Substage 5E conditions, respectively. The average late Holocene temperature at Hole 1002C, which is nearly identical to our box core composite modern temperature of 25.5°C, is 0.5°–1°C warmer than our reconstructed temperature at the LGM (Fig. 5). Similar patterns occurred from MIS 5 to 6. The small degree of glacial cooling inferred from alkenones is consistent with the dominance of *G. ruber* during the late glacial record observed by Peterson et al. (1991) but perhaps anomalous in light of oxygen isotope data, as discussed below.

Large, short-lived temperature anomalies seem to have occurred at glacial–interglacial transitions (Fig. 5). The ~3°C cooling coincides with the first signs of high alkenone abundance and the first laminated facies of the Holocene (Shipboard Scientific Party, 1997). It significantly precedes the interval correlated with Younger Dryas time, which does display alkenone temperatures ~1°C cooler than average Holocene values. The remainder of the Holocene shows modest temperature variations around the Holocene optimum of 25.8°C between 4 and 6 ka. A cooling of similar magnitude and duration identified at the MIS 5–6 transition occurs at a position stratigraphically identical to the well-defined temperature minimum reconstructed here at 13–14 ka (Fig. 4).

Very low alkenone concentrations consistently occur during MIS 2 and 4 (Fig. 4). The detailed record presented in Figure 5 shows that rather constant values were deposited from ~15–25 ka, despite the presence of laminated intervals (Shipboard Scientific Party, 1997). This interval also displays little variation in alkenone unsaturation index, an indication that the mixed oxic/anoxic conditions did not promote significant diagenetic alterations in the $U^{k'}_{37}$ index.

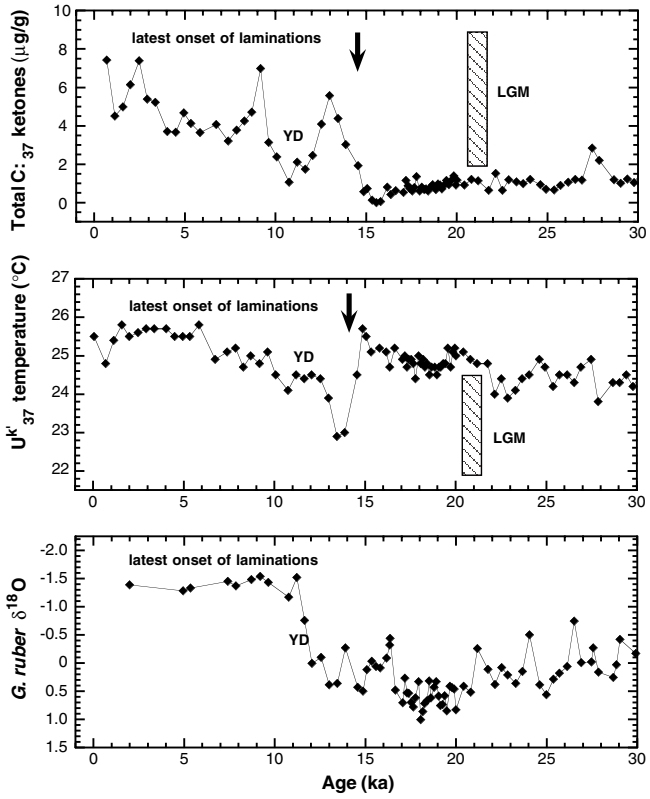

Figure 4. Alkenone records of concentration (µg/g dry sediment) and temperature estimated from the Prahl et al. (1988) relationship of unsaturation to growth temperature, compared to the oxygen isotopic record of *G. ruber* (Peterson et al., Chap. 4, this volume), on the Peterson et al. time scale. The arrows point to the location of the first laminated sediments in the Holocene from Hole 1002C, which corresponds to a spike of high alkenone concentration, high inferred paleoproductivity, and a short interval of cool surface waters. YD = the Younger Dryas Event, LGM = last glacial maximum.

SIGNIFICANCE OF THE ALKENONE RECORD

We assess next how to interpret alkenone results from Hole 1002C in light of oxygen isotope data and other constraints. Factors such as global changes in sea level, which regulate the depth of the sill connection between the Cariaco Basin and the open ocean; changes in local climate, including winds and freshwater runoff; and changes in regional surface temperatures and salinities all may affect the isotope and alkenone records to varying degrees. We do not expect salinity variations to influence the $U^{k'}_{37}$ temperature estimates (see Sonzogni et al., 1997), but they may indirectly modulate alkenone concentrations in the sediments by affecting patterns of inflow and outflow across the sills of the Cariaco Basin, and hence the nutrient and oxygen budgets of the basin. As Lin et al. (1997) point out, in the modern "estuarine" hydrography, the Cariaco Basin imports relatively nutrient-rich water at its sill depth of 146 m and exports nutrient-poor surface water into the open Caribbean (see also Richards, 1975). This circulation pattern promotes both high production of haptophyte algae in the water column and high preservation of alkenones in the sediments.

The alkenone concentration and paleotemperature estimates do not look very similar (see Figs. 4, 5). We assume the alkenone concentrations reflect haptophyte productivity, subject to possible influences of variable preservation and changing dilution by other sediment components (Villanueva et al., 1998). We have not converted our concentration estimates to fluxes because the order-of-magnitude changes in total C_{37} ketones that define the major Milankovitch-scale pattern (Fig. 4) are too large to explain by dilution/concentration mechanisms. The changes in ketone abundance must primarily reflect alterations in the production or preservation of these compounds over time. Furthermore, we are wary of introducing artifacts into the time series because of the potential error in correlating a planktonic isotope record with clear local influence with the global oxygen isotope time scale. As suggested above in our discussion of core-top alkenone paleotemperature analyses, we consider the $U^{k'}_{37}$ record to largely record changes in mean annual SST over the past 160 k.y. in the Cariaco Basin.

The lack of coupling between alkenone temperatures and amounts rules out simple interpretations of the data (e.g., that high upwelling rates result in cold temperatures). Instead, each data set has its own logic. Global sea level appears to have played a decisive role in controlling the time variations in alkenone concentration. As Figure 6 demonstrates, the alkenone abundances largely correlate with variations in total organic carbon. A model in which the sill depth sets the tendency of the Cariaco Basin to import nutrients and to establish bottom-water anoxia seems to explain most of the variations documented here. In addition, secondary effects (such as the intensity of upwelling-favorable winds) may have played a role in determining how productive and anoxic the Cariaco Basin became during sea-level highstands, setting variations like those seen in marine isotope Substages 5A and 5C above Holocene levels of alkenone concentration. One feature of note is the low variation in long-chain ketone abundance during marine isotope Stages 2, 4, and 6 relative to the remainder of the record. Alkenone concentrations remain uniformly low during these intervals, despite the frequent presence of "faint to well-developed" laminations (Shipboard Scientific Party, 1997). This may suggest very low variability in the exchange of waters across the shallow sills during glacial maxima. Significant fluctuations in alkenone concentration during MIS 3 and 4 may record intermittently greater connections to the open ocean during these intervals of somewhat higher sea level.

Two observations of the paleotemperature record over the full glacial cycle analyzed here seem particularly significant: the absence of cooling during the maximum extent of glaciation and the higher than modern temperatures inferred for Substage 5E. We first defend why the alkenone reconstructions of SST for the Cariaco Basin provide plausible results and then consider the implications for such an interpretation for isotopic data derived from *G. ruber*. To identify possible problems in interpreting the alkenone paleotemperature results, we must ask ourselves what factors might make at least some of the estimates unrepresentative. The most likely of these would be seasonal variations in alkenone synthesis and changes in the assemblage of alkenone-synthesizing haptophyte species. We believe that there is little basis for either objection in this setting.

To what degree could alkenone temperatures at Site 1002 be strongly biased by upwelling signals? This problem breaks down into two related questions: (1) Could variations in coastal upwelling be significant enough to produce SSTs in the Cariaco Basin unrepresentative of the open ocean? and (2) Could alkenone paleotemperatures be biased to record only upwelling conditions? First, in order to determine quantitatively by how much seasonal upwelling reduces the average temperature of Cariaco Basin, we can compare the magnitude of the upwelling effect in the basin to the adjacent open Caribbean Ocean. The two closest grid points from the World Ocean Atlas (Levitus, 1994) give identical values of 26.6°C, compared to our estimate of 25.1°C for Cariaco SST. Coastal upwelling therefore reduces annual SST in the Cariaco Basin by ~1.5°C relative to the open ocean; if upwelling were to shut off, SST would rise by about this amount. Decreased coastal upwelling during the last glacial period might mask some regional cooling in the Caribbean during the last glacial

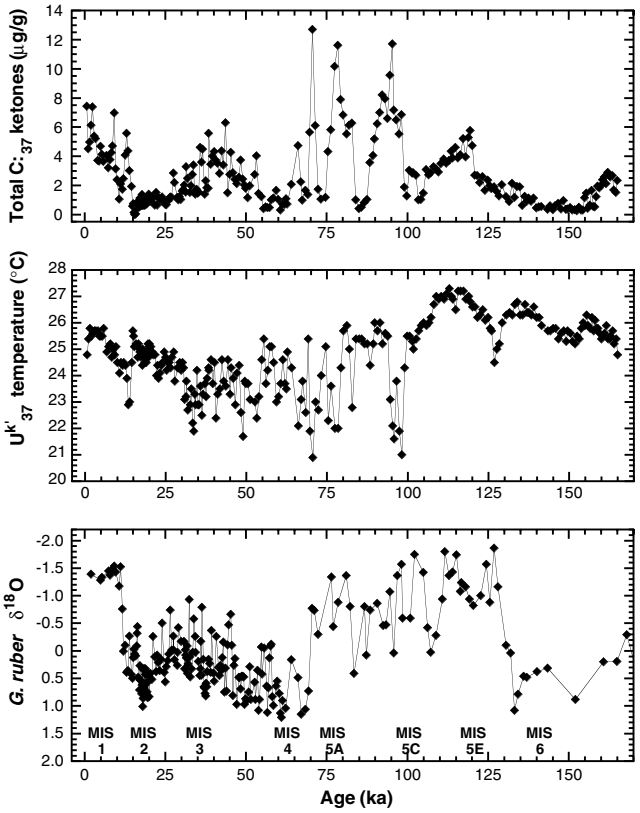

Figure 5. Detail of alkenone data over the last deglaciation (the most recent point comes from our box core composite). MIS = marine isotope stage/substage.

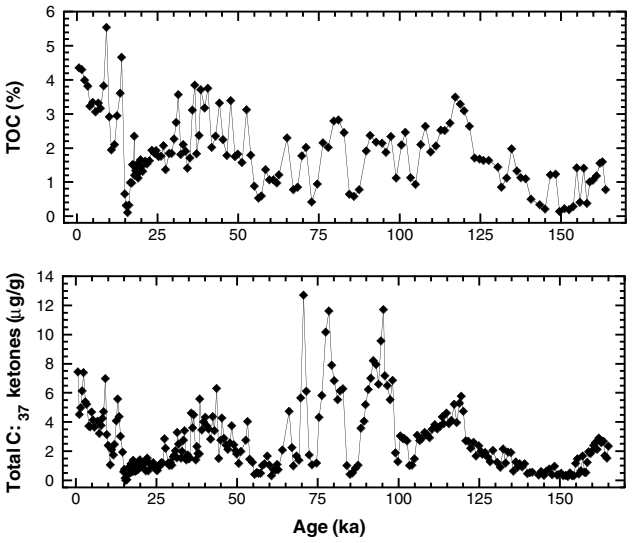

Figure 6. Comparison of total organic carbon (TOC) record (Haug et al., 1998) and the alkenone concentration data reported in this chapter. The similarities suggest that both variables largely record cyclic changes in surface production and in bottom-water anoxia.

period, but it could not by itself hide the 4°–5°C tropical cooling hypothesized by some (e.g., Guilderson et al., 1994).

There is also little basis to believe that alkenone temperatures are tightly correlated with upwelling temperatures, as we demonstrated above. Furthermore, alkenone temperatures do not deviate significantly from mean annual SST in other seasonal upwelling environments (Herbert et al., 1998). Our best present ecological understanding suggests that alkenone synthesis is fairly constant in tropical and mid-latitude settings, in part because haptophyte production may be suppressed by competition with diatoms during periods of peak export production (Holligan et al., 1993). We therefore conclude that although variations in upwelling intensity may provide a mechanism for changing SST and alkenone paleotemperatures in the Cariaco Basin on the order of 1°–2°C, they do not promote a strong bias toward the $U^{k'}_{37}$ signal.

Because alkenones appear to be produced within the mixed layer and with little seasonal bias in the late Holocene, past shifts in the depth of production could promote a bias toward $U^{k'}_{37}$ temperatures. This bias should be one-sided: the depth of production cannot shift upward relative to present-day conditions, but it could shift downward into the thermocline under different hydrographic conditions in the past. Examples of such subsurface production of alkenones and their cold bias have been documented for the North Pacific by Prahl et al. (1993). Note that this caveat does not affect our "warm" temperatures (like those observed during the LGM), but it could enter into some of the colder temperatures determined during intervals of MIS 3–5 (Figs. 4, 5).

Although $U^{k'}_{37}$ temperature offsets may occur between different strains or species of haptophyte algae (Volkman et al., 1995), core-top studies over large regions support the use of a single calibration function similar to the Prahl et al. (1988) culture study. This is true even in regions in which species such as *G. oceanica* form an important part of the nannofossil assemblage (Herbert et al., 1998; Müller et al., 1998).

Sea level and connections between the Cariaco Basin and the open ocean may have played a significant—and perhaps counterintuitive—role in determining glacial–interglacial changes in SST inferred from alkenone results. In this regard, we caution against interpreting our record as necessarily representative of regional patterns in SST. Consider how SST might be determined during sea-level lowstands. With a sill depth of ~26 m, the Cariaco Basin could not import waters colder than mixed-layer conditions in the Caribbean Sea (Lin et al., 1997). Temperatures below sill depth would be determined either by the temperature of this water or by production of deep water within the Cariaco Basin itself, perhaps influenced by seasonal or interannual salinity variations. In this situation, upwelling would have little, if any, efficiency in depressing SST because the thermocline would almost certainly be weak compared to the modern condition. More generally, a weakened thermocline would mean that all processes that act to mix the upper layers of Cariaco Basin would have had little impact on SST during sea-level lowstands.

Our explanation, then, pictures a basin during glacial maxima (which may have been much cooler than the Cariaco Basin) largely isolated from the open ocean. With relatively high insolation at its latitude of 10°N and few mechanisms to reduce SST, the Cariaco Basin may have been relatively buffered to glacial–interglacial variations in temperature. Swings to low SST occurred instead during intervals of somewhat higher sea level (such as during MIS 3–5C) and particularly during glacial terminations (see Fig. 5). At times of rising sea level, the deeper sill connections may have provided the cooler deep waters necessary to significantly lower SST compared to modern temperatures.

Such an interpretation presumes that colder SST characterized the open ocean outside the gates of the Cariaco Basin. There is no alkenone data at present to support this idea, and faunal studies suggest little if any cooling in the Caribbean during the LGM (CLIMAP, 1984). Cooling of 4°–5°C is supported by Sr/Ca values in corals (Guilderson et al., 1994) and by isotopic results from Andean ice cores (Thompson et al., 1995). The alkenone results presented here may or may not represent a regional or local response of surface temperatures to glacial–interglacial climate change.

If our alkenone temperature estimates are correct, they imply substantial evaporation/precipitation/runoff contributions to the *G. ruber* oxygen isotopic record of Peterson et al. (Chap. 4, this volume). The glacial–interglacial isotopic amplitude of ~2.2‰ requires a significant combination of temperature and/or salinity effects compared with the global ice-volume effect of 0.9‰–1.2‰ (Fairbanks and Matthews, 1978; Schrag et al., 1996). Very short-lived excursions of 1‰ or more during MIS 3–5C also require nonglobal influences on the surface isotopic record from the Cariaco Basin. We caution against point-by-point comparison of the alkenone and isotopic time series because samples are generally offset by tens of centimeters and because both data sets display high-frequency variations. Nevertheless, the alkenone paleotemperatures imply that ~1‰ of the glacial enrichment in oxygen isotopic composition of *G. ruber* must be caused by changes in the local runoff and evaporation/precipitation balance. This would require an increase in salinity at the LGM of ~2‰ using standard salinity $\delta^{18}O$ correlations (Craig and Gordon, 1965) and/or a reduction of local runoff whose effect on modern surface $\delta^{18}O$ values in the Cariaco Basin is not quantified.

This interpretation of the Cariaco $\delta^{18}O$ record is plausible but is not without problems. Lin et al. (1997) set an excellent standard for balancing the case for a favored model and considering objections to this model in order to explain variations in planktonic $\delta^{18}O$. They documented the large amplitude of the *G. ruber* $\delta^{18}O$ signal from the LGM to the Holocene in the Cariaco Basin. In addition, the authors demonstrated that the foraminifers *G. bulloides* (an upwelling species) and *N. dutertrei* (representing deeper water conditions) display glacial–interglacial changes of only ~1.3, or nearly the expected ice-volume effect alone. Lin et al. (1997) interpreted the large enrichment in *G. ruber* isotopic values at the LGM to represent a 4°–5°C cooling of surface waters. They noted at the same time that the absence of isotopic enrichment in the other foraminiferal species raises problems in this interpretation. First, one would expect that bottom waters in the Cariaco Basin would actually have warmed during the LGM because the basin could not be ventilated by waters much below the mixed layer. This warming ought to partially offset the global ice-volume signal in the *G. bulloides* and *N. dutertrei* records. Second, if all of the *G. ruber* isotopic variance comes from cooling during the last glacial period, one obtains a reconstruction of a thermally homogeneous upper water column (for example, one can superimpose a 4°–5°C cooling at the surface on the profile shown in Fig. 2).

Our model reconciles isotopic results with alkenone paleotemperature estimates by requiring much higher salinities in the Cariaco Basin during sea-level lowstands than are found today. A large fraction of the salinity signal in this region today apparently originates from advection of Orinoco and Amazon discharges (Dessier and Donguy, 1994), which are modulated by the passage of the Intertropical Convergence Zone (ITCZ) (Hastenrath, 1990). Higher salinities during the glacial period would result from the greater physical isolation of Cariaco waters from the open ocean, from regional reductions in rainfall as ITCZ failed to advance as far northward as it does today, and from reduced freshwater input into the Cariaco Basin from local tributaries and from the major South American river systems. This model would require large changes in surface salinity but permit a combination of temperature and salinity variations at the depth and seasons represented by the *G. bulloides* and *N. dutertrei* records of Lin et al. (1997). In the latter examples, the isotopic effects of warmer deep waters and higher salinities may have canceled each other out, leaving the global ice-volume signal as the residual.

Several independent lines of evidence support this interpretation. Faunal studies fail to indicate surface cooling in Cariaco Basin sedi-

ments or in the adjacent Caribbean (CLIMAP, 1984; Lin et al., 1997). Planktonic foraminiferal faunas during the LGM are dominated by the tropical species *G. ruber* (Overpeck et al., 1989). Unusual benthic assemblages in the Cariaco Basin are similar to those found in abnormally high-salinity environments (Peterson et al., Chap. 4, this volume). Studies of the terrestrial paleoenvironment point to greater aridity in the region (Leyden, 1984, 1985; Margraf, 1989).

Our alkenone unsaturation time series also suggests that SST warmed during marine isotope Substage 5E to ~2°C warmer than present temperatures (Fig. 4). The unsaturation values lie near the end of the analytical range of the $U^{k'}_{37}$ index and past the highest growth temperature used by Prahl et al. (1988) in their culture calibration of the $U^{k'}_{37}$ index. Warmer than Holocene values for Substage 5E at Site 1002 are consistent with other alkenone determinations at open ocean locations, as follows: 1.5°C warmer in the northwest Arabian Sea (Emeis et al., 1995), 1°C warmer in the equatorial Atlantic, 1.5°C warmer at 11°S in the South Atlantic, 1.5°C warmer off the Congo Fan, 1.5°C warmer along the Angola Margin, 4°C warmer at the Walvis Ridge (Schneider et al., 1995), 3.5°C warmer in the tropical North Atlantic (Eglinton et al., 1992), 4°C warmer in Santa Barbara Basin (Herbert et al., 1995), and 3°C warmer in the North Pacific at ODP Site 1020 (S. Kreitz, unpubl. data).

In the end, studies like those reported here will have to be interpreted in light of similar records from the open Caribbean Ocean. The oceanography of the Cariaco Basin and its sensitivity to sea-level variations are unusual enough to make us cautious in inferring more than local significance to our alkenone time series. The presence of laminated sediments and high accumulation rates in the Cariaco Basin thus presents something of a paradox. Do they represent an unusual opportunity to observe the sensitivity of a tropical climate to global changes, or a system so highly amplified as to be unrepresentative of the open tropical ocean? Studies of oxygen-isotopic amplitude during the LGM from the tropical Atlantic are mixed: Curry and Oppo (1997) documented large anomalies from the Ceara Rise, whereas Stott and Tang (1996) found shifts consistent with only minimal cooling of surface waters. Milankovitch-scale sampling for $\delta^{18}O$ and alkenone paleotemperatures on pelagic cores outside the Cariaco Basin are needed to determine whether the general glacial–interglacial features presented here are representative of the region (in which case the high-frequency isotopic and $U^{k'}_{37}$ variations documented by Peterson et al. [Chap. 4, this volume] take on added significance) or whether the paleoceanography of the Cariaco Basin is largely a story of contrasts between the basin and the open ocean.

ACKNOWLEDGMENTS

We thank Dr. F. Müller-Karger for sharing Cariaco hydrographic time series data with us. We also thank Drs. G. Haug and L. Peterson for sharing sediment data with us ahead of publication, Dr. D. Murray for providing us with box core sediment samples from the Plume-07 cruise, and Dr. M. Goni and an anonymous reviewer for improving the manuscript.

REFERENCES

Bond, G.C., Broecker, W.S., Johnsen, S., McManus, J., Labeyrie, L., Jouzel, J., and Bonani, G., 1993. Correlations between climate records from North Atlantic sediments and Greenland ice. *Nature,* 366:552–554.

Brassell, S.C., 1993. Applications of biomarkers for delineating marine paleoclimatic fluctuations during the Pleistocene. *In* Engel, M.H., and Macko, S.A. (Eds.), *Organic Geochemistry: Principles and Applications:* New York (Plenum), 699–738.

Broecker, W.S., 1986. Oxygen isotope constraints on surface ocean temperatures. *Quat. Res.*, 26:121–134.

CLIMAP Project Members, 1976. The surface of the ice-age Earth. *Science,* 191:1131–1137.

————, 1984. Seasonal reconstruction of the earth's surface at the last glacial maximum. Geol. Soc. Am. Map Chart Ser., MC-36.

Craig, H., and Gordon, L.I., 1965. Deuterium and oxygen-18 variations in the ocean and the marine atmosphere. *In* Tongiorgi, E. (Ed.), *Stable Isotopes in Oceanographic Studies and Paleotemperatures:* Pisa (Cons. Naz. delle Ric., Lab. di Geol. Nucleare), 9–130.

Curry, W.B., and Oppo, D.W., 1997. Synchronous, high-frequency oscillations in tropical sea surface temperatures and North Atlantic Deep water production during the last glacial cycle. *Paleoceanography*, 12:1–14.

Dessier, A., and Donguy, J.R., 1994. The sea surface salinity in the tropical Atlantic between 10°S and 30°N: seasonal and interannual variations (1977–1989). *Deep Sea Res.,* 41:81–100.

Eglinton, G., Bradshaw, S.A., Rosell, A., Sarnthein, M., Pflaumann, U., and Tiedemann, R., 1992. Molecular record of secular sea surface temperature changes on 100-year timescales for glacial terminations I, II, and IV. *Nature,* 356:423–426.

Emeis, K.-C., Anderson, D.M., Doose, H., Kroon, D., and Schulz-Bull, D., 1995. Sea-surface temperatures and the history of monsoon upwelling in the northwest Arabian Sea during the last 500,000 years. *Quat. Res.,* 43:355–361.

Fairbanks, R.G., 1989. A 17,000-year glacio-eustatic sea level record: influence of glacial melting rates on the Younger Dryas event and deep-ocean circulation. *Nature,* 342:637–642.

Fairbanks, R.G., and Matthews, R.K., 1978. The marine oxygen isotope record in Pleistocene coral, Barbados, West Indies. *Quat. Res.,* 10:181–196.

Guilderson, T.P., Fairbanks, R.G., and Rubenstone, J.L., 1994. Tropical temperature variations since 20,000 years ago: modulating interhemispheric climate change. *Science*, 263:663–665.

Hastenrath, S., 1990. Diagnostic and prediction of anomalous river discharge in northern South America. *J. Climate,* 3:1080–1096.

Haug, G.H., Pedersen, T.F., Sigman, D.M., Calvert, S.E., Nielsen, B., and Peterson, L.C., 1998. Glacial/interglacial variations in production and nitrogen fixation in the Cariaco Basin during the last 580 kyr. *Paleoceanography*, 13:427–432.

Herbert, T.D., Schuffert, J.D., Thomas, D., Lange, K., Weinheimer, A., and Herguera, J.-C., 1998. Depth and seasonality of alkenone production along the California margin inferred from a core-top transect. *Paleoceanography,* 13:263–271.

Herbert, T.D., Yasuda, M., and Burnett, C., 1995. Glacial-interglacial sea-surface temperature record inferred from alkenone unsaturation indices, Site 893, Santa Barbara Basin. *In* Kennett, J.P., Baldauf, J.G., and Lyle, M. (Eds.), *Proc. ODP, Sci. Results*, 146 (Pt. 2): College Station, TX (Ocean Drilling Program), 257–264.

Herrera, L.E., and Febres-Ortega, G., 1975. Procesos de surgencia y de renovacion de aguas en la Fosa de Cariaco, Mar Caribe. *Bol. Inst. Oceanogr., Univ. Oriente,* 14:31–44.

Holligan, P.M., Groom, S.B., and Harbour, D.S., 1993. What controls the distribution of the coccolithophore, *Emiliania huxleyi,* in the North Sea? *Fish. Oceanogr.,* 2:175–183.

Hughen, K., Overpeck, J.T., Peterson, L.C., and Trumbore, S.E., 1996. Rapid climate changes in the tropical Atlantic region during the last deglaciation. *Nature*, 380:51–54.

Lesley, D., Conte, M.H., Thompson, A., Harris, R.P., and Eglinton, G., 1996. Calibration of the alkenone/alkenoate temperature signal in selected *E. huxleyi* and *Gephyrocapsa oceanica* strains from different oceanic regions. *Eos,* 76:149.

Levitus, S., 1994. Climatological atlas of the world ocean. *NOAA Prof. Pap.,* 13.

Leyden, B.W., 1984. Guatemalan forest synthesis after Pleistocene aridity, *Proc. Nat. Acad. Sci. USA,* 81:4856–4859.

————, 1985. Late Quaternary aridity and Holocene moisture fluctuations in the Lake Valencia basin, Venezuela. *Ecology,* 66:1279–1295.

Lin, H.-L., Peterson, L.C., Overpeck, J.T., Trumbore, S.E., and Murray, D.W., 1997. Late Quaternary climate change from $\delta^{18}O$ records of multiple species of planktonic foraminifera: high-resolution records from the anoxic Cariaco Basin (Venezuela). *Paleoceanography*, 12:415–427.

Lyle, M., Prahl, F.G., and Sparrow, M.A., 1992. Upwelling and productivity changes inferred from a temperature record in the central equatorial Pacific. *Nature,* 355:812–815.

Margraf, V., 1989. Palaeoclimates in the Central and South America since 18,000 BP based on pollen and lake-level records. *Quat. Sci. Rev.,* 8:1–24.

Marlowe, I.T., Brassell, S.C., Eglinton, G., and Green, J.C., 1984. Long-chain unsaturated ketones and esters in living algae and marine sediments. *In* Schenck, P.A., de Leeuw, J.W., and Lijmbach, G.W.M. (Eds.), *Advances in Organic Geochemistry 1983*. Org. Geochem., 6:135–141. Mix, A.C., Ruddiman, W.F., and McIntyre, A., 1986. The late Quaternary paleoceanography of the tropical Atlantic. 1: Spatial variability of annual mean sea-surface temperatures, 0–20,000 years B.P. *Paleoceanography,* 1:43–66.

Müller, P.J., Kirst, G., Ruhland, G., von Storch, I., and Rossell-Mele, A., 1998. Calibration of the alkenone paleotemperature index $U^{k'}_{37}$ based on core-tops from the eastern South Atlantic and the global ocean (60°N-60°S). *Geochim. Cosmochim. Acta,* 62:1757–1772.

Overpeck, J.T., Peterson, L.C., Kipp, N., Imbrie, J., and Rind, D., 1989. Climate change in the circum-North Atlantic region during the last deglaciation. *Nature*, 338:553–557.

Peterson, L.C., Overpeck, J.T., Kipp, N.G., and Imbrie, J., 1991. A high-resolution late Quaternary upwelling record from the anoxic Cariaco Basin, Venezuela. *Paleoceanography,* 6:99–119.

Prahl, F.G., Collier, R.B., Dymond, J., Lyle, M., and Sparrow, M.A., 1993. A biomarker perspective on prymnesiophyte productivity in the northeast Pacific Ocean. *Deep-Sea Res. Part A*, 40:2061–2076.

Prahl, F.G., Muehlhausen, L.A., and Lyle, M., 1989. An organic geochemical assessment of oceanographic conditions at MANOP Site C over the past 26,000 years. *Paleoceanography,* 4:495–510.

Prahl, F.G., Muehlhausen, L.A., and Zahnle, D.L., 1988. Further evaluation of long-chain alkenones as indicators of paleoceanographic conditions. *Geochim. Cosmochim. Acta,* 52:2303–2310.

Prahl, F.G., and Wakeham, S.G., 1987. Calibration of unsaturation patterns in long-chain ketone compositions for paleotemperature assessment. *Nature,* 330:367–369.

Richards, F.A., 1975. The Cariaco Basin (Trench). *Annu. Rev. Oceanogr. Mar. Biol.,* 13:11–67.

Rind, D., and Peteet, D., 1985. Terrestrial conditions at the last glacial maximum and CLIMAP sea-surface temperature estimates: are they consistent? *Quat. Res.,* 24:1–22.

Rossell-Mele, A., Carter, J., and Eglinton, G., 1994. Distribution of long-chain alkenones and alkyl alkenoates in marine surface sediments from the North East Atlantic. *Org. Geochem.,* 22:501–509.

Schneider, R.R., Müller, P.J., and Ruhland, G., 1995. Late Quaternary surface circulation in the east equatorial Atlantic: evidence from alkenone sea surface temperatures. *Paleoceanography,* 10:197–219.

Schrag, D.P., Hampt, G., and Murray, D.W., 1996. The temperature and oxygen isotopic composition of the glacial ocean. *Science,* 272:1930–1932.

Shipboard Scientific Party, 1997. Site 1002. *In* Sigurdsson, H., Leckie, R.M., Acton, G.D., et al., *Proc. ODP, Init. Repts*., 165: College Station, TX (Ocean Drilling Program), 359–373.

Sikes, E.L., Farrington, J.W., and Keigwin, L.D., 1991. Use of the alkenone unsaturation ratio Uk-37 to determine past sea surface temperatures: core-top SST calibrations and methodology considerations. *Earth Planet. Sci. Lett.,* 104:36–47.

Sonzogni, C., Bard, E., Rostek, F., Dollfus, D., Rosell-Mele, A., and Eglinton, G., 1997. Temperature and salinity effects on alkenone ratios measured in surface sediments from the Indian Ocean. *Quat. Res.,* 47:344–355.

Stott, L.D., and Tang, C.M., 1996. Reassessment of foraminiferal-based tropical sea surface $\delta^{18}O$ paleotemperatures. *Paleoceanography,* 11:37–56.

Thompson, L.G, et al., 1995. Late glacial stage and Holocene tropical ice core records from Huascaran, Peru. *Science,* 269:46–50.

Villanueva, J., Grimalt, J.O., Labeyrie, L., Cortijo, E., Vidal, L., and Turon, J.-L., 1998. Precessional forcing of productivity in the North Atlantic Ocean. *Paleoceanography,* 13:561–571.

Volkman, J.K., Barrett, S.M., Blackburn, S.I., and Sikes, E.L., 1995. Alkenones in Gephyrocapsa oceanica: implications for studies of paleoclimate. *Geochim. Cosmochim. Acta,* 59:513–520.

Volkman, J.K., Eglinton, G., Corner, E.D.S., and Sargent, J.R., 1980. Novel unsaturated straight-chain C_{37}–C_{39} methyl and ethyl ketones in marine sediments and a coccolithophore *Emiliania huxleyi. In* Douglas, A.G., and Maxwell, J.R. (Eds.), *Advances in Organic Geochemistry 1979:* Oxford (Pergamon Press), 219–228.

Date of initial receipt: 27 July 1998
Date of acceptance: 29 April 1999
Ms 165SR-030